Available online at www.sciencedirect.com
SCIENCE DIRECT
Polymer 47 (2006) 2116–2126
polymer
www.elsevier.com/locate/polymer

Isothermal crystallization and melting behaviors of nylon 11/nylon 66 alloys by in situ polymerization

Xikui Zhang [a], Tingxiu Xie [c], Guisheng Yang [b,c,*]

[a] Material Science and Engineering Institute, East China University of Science and Technology, Shanghai 200237, People's Republic of China
[b] CAS Key Laboratory of Engineering Plastics, Joint Laboratory of Polymer Science and Materials, Institute of Chemistry, Chinese Academy of Sciences, Beijing 100080, People's Republic of China
[c] Research and Development Center, Shanghai Genius Advanced Materials Co., Ltd, Shanghai 201109, People's Republic of China

Received 28 September 2005; received in revised form 19 January 2006; accepted 22 January 2006

Abstract

Nylon 11/nylon 66 alloys were prepared by in situ polymerization. Analysis of the isothermal crystallization behaviors of nylon 11/nylon 66 alloys was carried out using differential scanning calorimetry (DSC) and X-ray diffraction (XRD). The crystallization kinetics of the primary stage under isothermal conditions could be described by the Avrami equation. The crystal morphology observed by means of polarized optical microscope (POM). In the DSC scan after isothermal crystallization process, the multiple melting behaviors were found and each melting endotherm has a different origin. The real-time XRD measurements confirmed that no crystalline transition existed during the isothermal crystallization process. The multiple endotherms were experimentally evidenced due to melting of the recrystallizated materials or the lamellae produced under different crystallization processes. The equilibrium melting point of samples for isothermal crystallization was also evaluated.

Keywords: Crystallization; Nylon 11; Alloys

1. Introduction

It is well known that the physical, chemical and mechanical properties of crystalline polymers depend on the morphology, the crystalline structure and the degree of crystallization. Meanwhile, the crystallization process dramatically affects the crystal structure and morphology established during the solidification process. In order to control the rate of the crystallization and the degree of crystallinity and to obtain the desired morphology and properties, a great deal of effort has been devoted into studying the crystallization kinetics and determining the change in material properties [1–3]. Additionally, crystallization behavior represents an interesting research subject in order to optimize process conditions and control the properties of the final products.

Nylon 11 is an important polymer used in a large range of industrial fields from automotive to offshore applications, which derives from its excellent piezoelectric behavior, good cryogenic, oil resistance and water resistance properties [4–10]. Research is often focusing on its crystal structure and morphology characteristics [11–16] and its modification through blending [4,17–19], while its modification in its molecular structure has received little attention. In this work, we use nylon 66 to modify nylon 11 by in situ polymerization. Nylon 11 and nylon 66 are not completely miscible in nature, although nylon 11/nylon 66 alloys can be prepared via a solution blending of components, phase separation may occur during practical processing. A possible solution to this problem is to dissolve nylon 66 polymer in nylon 11 monomers, 11-aminoundecanoic acid, which can be later polymerized as a matrix. These alloys cannot uniformly disperse in matrix, but might also obtain improved mechanical properties with strong interfacial adhesion. The crystallization of nylon 11 in the alloys is often influenced not only by the processing conditions, but also by the nylon 66.

In this paper, the isothermal crystallization behaviors of nylon 11/nylon 66 alloys were carried out by differential scanning calorimetry (DSC); the melting behaviors following isothermal crystallization process were also discussed. Several kinetics methods were applied to analyze its isothermal crystallization process. The crystal structure was characterized by real-time X-ray diffraction (XRD). The crystal morphology was observed by means of polarized optical microscope

* Corresponding author. Tel.: +86 21 648 81869; fax: +86 21 649 06922.
E-mail address: ygs@geniuscn.com (G. Yang).

0032-3861/$ - see front matter © 2006 Elsevier Ltd. All rights reserved.
doi:10.1016/j.polymer.2006.01.077

(POM). The equilibrium melting point for isothermal crystallization of alloys has also been evaluated according to the classical theory.

2. Experimental

2.1. Materials preparation

The monomer was 11-aminoundecanoic acid (ACROS ORGANICS). Clear nylon 66 without any additives was supplied by China ShenMa Group Co., Ltd, with M_w = 26,000 g/mol, $M_w/M_n = 1.85$. The samples of nylon 11/nylon 66 alloys were prepared by in situ polymerization. Synthesis procedures were as follows: at first, 11-aminoundecanoic acid was mixed with nylon 66 polymer in a vessel with the contents of 5 and 10 wt%, respectively, and the mixture was heated under a nitrogen atmosphere to 180–200 °C while the pressure was increased to 0.8 MPa, and then kept constant for 1 h; secondly, the mixture was again heated to 230–260 °C and kept 3 h to achieve polymerization; finally, the pressure began to level off, and the reaction was further carried out at atmospheric pressure for 0.5–1 h and got the resulting alloys. For purpose of comparison, the neat nylon 11 was synthesized by the same procedure. According to Ref. [20], the products of nylon 11 contains little monomer or oligomers and need not further extraction. The purity of nylon 11 was confirmed by NMR, there was not discernable trace of impurities. It is also in consistent with the Ref. [20]. The neat nylon 11 is abbreviated as N-0A; similarly, the nylon 11/nylon 66 alloys containing 5 and 10 wt% nylon 66 are abbreviated as N-5A and N-10A, respectively.

The nylon 11/nylon 66 blends were prepared by melt extrusion in a corotating twin-screw extruder ($\Phi = 35$ mm, SHJ-30) at 240 rpm. The barrel temperatures were 230–250 °C. Nylon 11 is our synthetic product; nylon 66 is the same product as above.

2.2. Gel permeation chromatograms (GPC)

A Waters-991 GPC instrument was used to evaluate the weight-average molecular weight (M_w) of samples and their polydispersities (M_w/M_n), where M_n is the number-average molecular weight. The final quantities were determined using the calibration curve of narrow distribution nylon 6 standards. The measurements were performed at 35 °C on polymeric solutions in *m*-cresol. Before measurements, the samples were dried under vacuum at 80 °C for 12 h.

2.3. Differential scanning calorimetry

Crystallization process was carried out using a Perkin–Elmer Diamond DSC. Calibration was carried out by using an indium standard, with accuracy of temperature control being ±0.01 °C. All DSC experiments were performed under a nitrogen purge at a constant flow rate; the sample weights were between 5 and 6 mg.

The samples were prepared using compression-molding at a temperature of 230 °C with a pressure of 10 MPa for 5 min, and then gradually cooled to the room temperature. The samples were dried under vacuum at 80 °C for 12 h before measurements.

2.3.1. Nonisothermal crystallization process

The sample N-10A was rapidly heated at a rate of 80 °C/min to 280 °C, stayed there for 10 min to eliminate any residual crystals, and then cooled to 50 °C at different cooling rates of 2.5, 5, 10, 20, and 40 °C/min.

2.3.2. Isothermal crystallization process

The samples were rapidly heated at a rate of 80 °C/min to 230 °C above the melting temperature, stayed there for 10 min to eliminate any residual crystals, and then rapidly cooled to the designated crystallization temperature (T_c) at a rate of 80 °C/min, which were five different temperatures in the range of 154–172 °C for each sample in the isothermal crystallization process, and held at this temperature for 30 min until crystallization was complete. The specimens were subsequently heated to 230 °C at a rate of 10 °C/min.

For a better definition of the beginning time of crystallization, for each isothermal scan blank runs were also performed with the same sample. The blank run was subtracted from the isothermal crystallization scan and the start of the process was taken as the intersection of the extrapolated baseline and the resulting exothermal curve [21,22].

2.4. Polarized optical microscope

The crystallite morphologies were observed by a LEICA DMLP POM equipped with a Linkam TMS94 hot stage. The film samples (with thickness of 10 μm) were prepared by compression molding in a press at a temperature of 230 °C and with a pressure of 150 bar, then gradually cooled to the room temperature. The samples, placed on glass slides covered with slips, were rapidly heated to 230 °C to melt and held at this temperature for 5 min to eliminate any thermal and mechanical history, then cooled rapidly to the designated temperature for isothermal crystallization observations. Dry nitrogen gas was purged through the hot stage in all measurement processes.

2.5. X-ray diffraction

The X-ray diffraction (XRD) measurements were obtained in a Rigaku D/MAX 2500 diffractometer with curved graphite crystal filtered. The corresponding wide-angle X-ray diffraction patterns were collected in transmission mode at room temperature operating under a tube current of 40 mA and an acceleration voltage of 40 kV, using Cu Kα radiation (λ = 0.154056 nm). The scanning rate was 4°/min.

In real-time measurements, sample plates with dimensions $1 \times 1 \times 0.05$ cm^3 were prepared using two hot compression molding in a press at a temperature of 230 °C and then gradually cooled to the room temperature. The samples were pretreated as same as DSC samples before measurements. During the measurements the sample was protected by a flow of inert gas (helium) to prevent the oxidation at high

temperatures. The sample was placed in a platinum block sample holder and heated at the rate of 10 °C/min to the desired temperature. A waiting time of 5 min was given after the system arrived at the respective temperature in order to reach a relative equilibrium state and allowed the diffractograms to be recorded.

3. Results and discussion

3.1. Characteristic of samples

Nylon 11 and nylon 66 by blending are not completely miscible in nature, the DSC traces of nylon 11 and nylon 66 blending can confirm it in Fig. 1, the cooling and the second heating rate is 10 °C/min. It can be seen that the DSC thermograms have the distinct melting temperature of nylon 11 and nylon 66, respectively. The DSC traces of samples prepared by in situ polymerization are presented in Fig. 2, the cooling and the second heating rate is also 10 °C/min. It is clear that there is no characteristic melting or crystallization peak of nylon 66. So the nylon 66 was completely miscible in the nylon 11 matrix through in situ polymerization mode. In order to confirm it, a nonisothermal test was also made, as shown in Fig. 3. It is clear that there is no characteristic melting or crystallization peak of nylon 66.

From Fig. 2, it can be seen that the alloy's melting temperature is lower than that of neat nylon 11. So the temperature for isothermal crystallization experiments was only heated to 230 °C above the melting temperature.

The influence of molecular weight on the crystallization together with a comparison with multiple melting traces was first reported by Gurato et al. [23]. The similar study was reported in Nylon 6 [24] and in PET [25,26]. The purpose of the present study is to analyze the general characteristics of crystallization and melting for nylon 11/nylon 66 alloys and to show that the complex influence of nylon 66 on nylon 11 crystallization. Therefore, we controlled the molecular weight

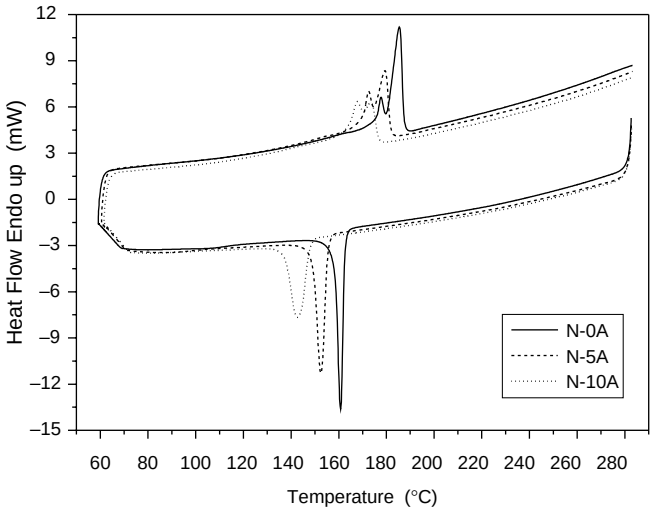

Fig. 2. The DSC thermograms of samples: N-0A is neat nylon 11; N-5A is alloy containing 5 wt% nylon 66; N-10A is alloy containing 10 wt% nylon 66.

of samples as uniformly as possible to eliminate the possible effect on crystallization through synthetic process. The weight-average molecular weight and its distribution of samples are shown in Fig. 4. In the present study, we are considering samples as quiescent materials; therefore, correlations with the indicated results would only be possible under such conditions.

3.2. Isothermal crystallization behaviors

The crystallization behaviors of samples were studied by DSC. Fig. 5 shows the DSC traces for samples that had been isothermally crystallized at different temperatures. Because the melting temperatures of samples are different, the isothermal crystallization temperature ranges are different for each sample. The chosen crystallization temperature was determined through a series of experiments conducted at various crystallization temperatures. In Fig. 5, the exothermic flows

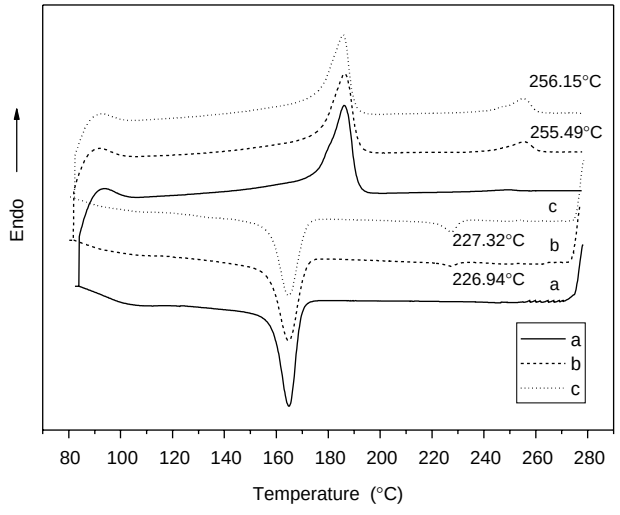

Fig. 1. The cooling and second heating traces of nylon 11/nylon 66 blending: (a) neat nylon 11; (b) nylon 11/nylon 66 (95/5 wt%); (c) nylon 11/nylon 66 (90:10 wt%).

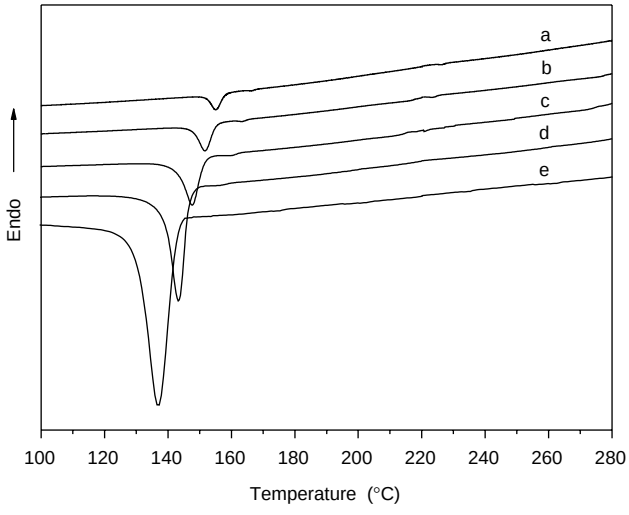

Fig. 3. The DSC thermograms of nontisothermal crystallization of N-10A at different cooling rates of (a) 2.5 °C/min; (b) 5 °C/min; (c) 10 °C/min; (d) 20 °C/min; (e) 40 °C/min.

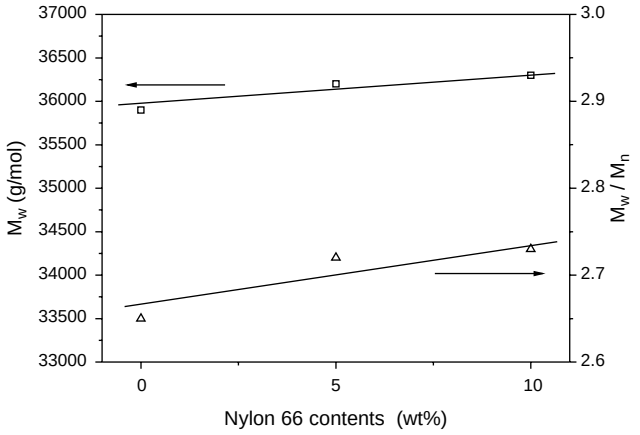

Fig. 4. The weight-average molecular weight (M_w) and distribution (M_w/M_n) of samples by in situ polymerization.

caused by the cooling rate change had been separated on the numerical integrations.

From Fig. 5, it can be seen that the crystallization peaks shift to the right and become flatter with increasing crystallization temperature. It implies that the sample requires a longer time to complete crystallization with higher crystallization temperature, and the crystallization rate decreases with increasing the crystallization temperature. Due to the decrease of the supercooling temperature ($\Delta T = T_m^0 - T_c$), the crystallization time becomes longer and the crystallization rate decreases. Meanwhile, the crystallization peaks shift to lower temperatures with the addition of nylon 66.

In the study, the relative degree of crystallinity at time t, $X(t)$, is defined as follows [27]:

$$X(t) = \frac{X_c(t)}{X_c(t\infty)} = \frac{\int_0^t \frac{dH(t)}{dt} dt}{\int_0^{t\infty} \frac{dH(t)}{dt} dt} = \frac{\Delta H_t}{\Delta H_\infty} \quad (1)$$

where dH/dt is the rate of heat evolution; ΔH_t is the heat generated at time t; ΔH_∞ is the total heat generated up to the end of the crystallization process. Fig. 6 shows the relative crystallinity at different crystallization time in the process of isothermal crystallization. It can be seen that characteristic sigmoid isotherms shift to the right with increasing isothermal crystallization temperature, and the crystallization rate becomes slower.

Assuming the relative degree of crystallinity increases with an increase of crystallization time, the Avrami equation [28] can be used to describe the isothermal crystallization behavior. The Avrami equation is given as follows:

$$X(t) = 1 - \exp(-Kt^n) \quad (2a)$$

$$\log\{-\ln[1 - X(t)]\} = n \log t + \log K \quad (2b)$$

where n is a constant that depends on the type of nucleation and growth of the crystals; K is the crystallization rate constant involving both nucleation and growth rate parameters under isothermal conditions. Usually, the values of n should be an integer between 1 and 4 for different crystallization mechanisms. Since other complex factors, such as the competition of

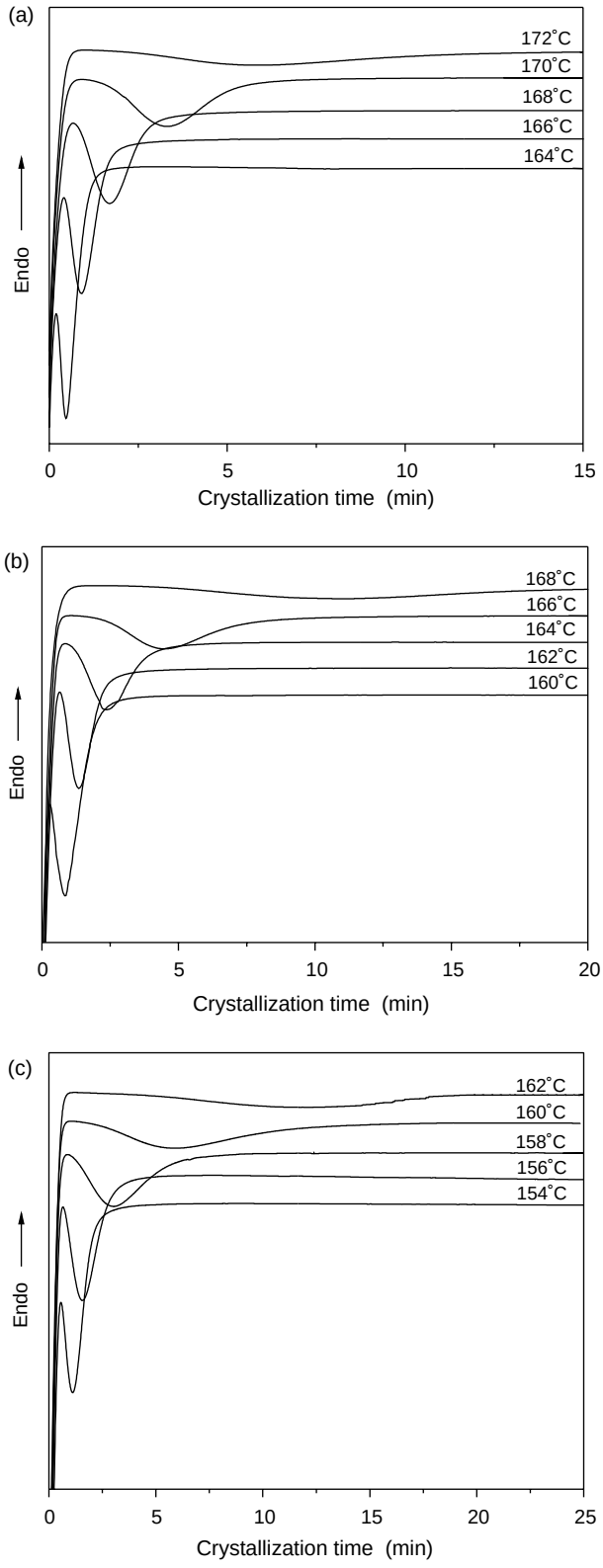

Fig. 5. The DSC traces of samples isothermally crystallized at the specified temperatures: (a) N-0A; (b) N-5A; (c) N-10A.

a diffusion-controlled growth and/or to the irregular boundary of the spherulites, are probably involved during the process, the Avrami exponent n is not a straightforward integer [29]. By plotting $\log\{-\ln[1 - X(t)]\}$ versus $\log t$, we can obtain K and n

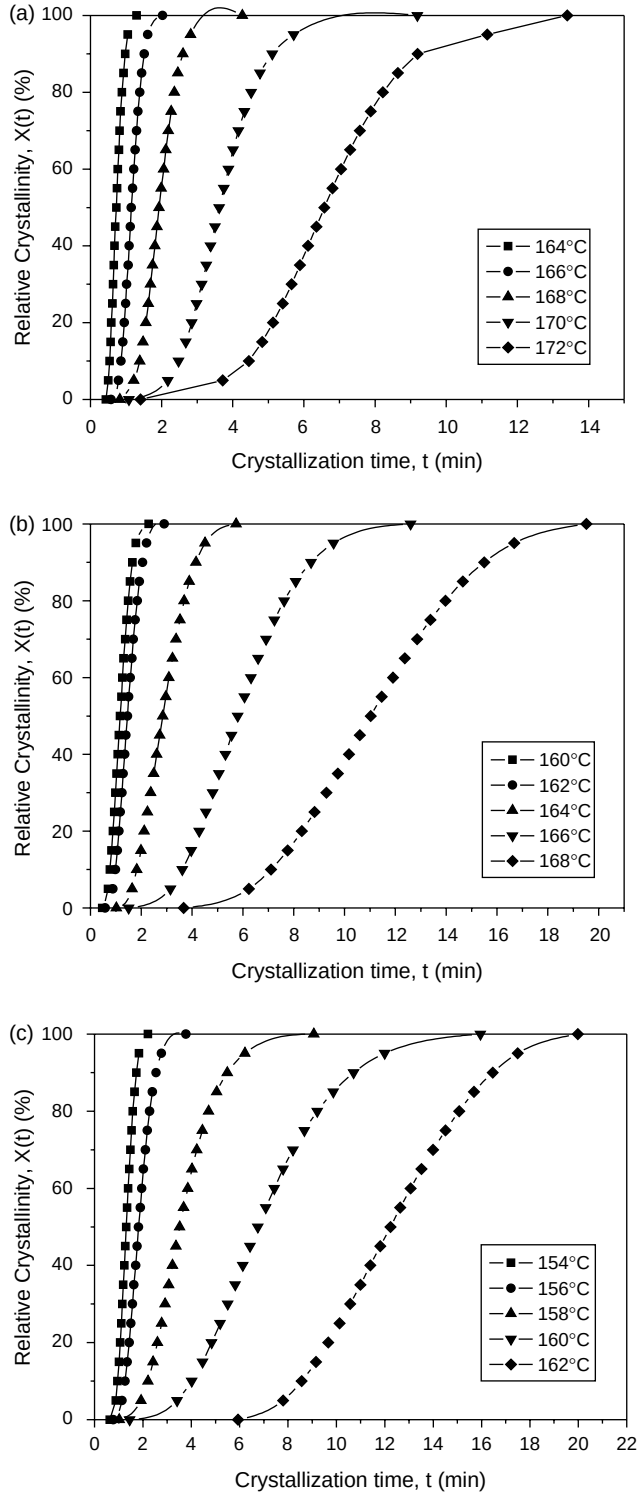

Fig. 6. Relative crystallinity $X(t)$ versus different crystallization time t in the process of isothermal crystallization for samples: (a) N-0A; (b) N-5A; (c) N-10A.

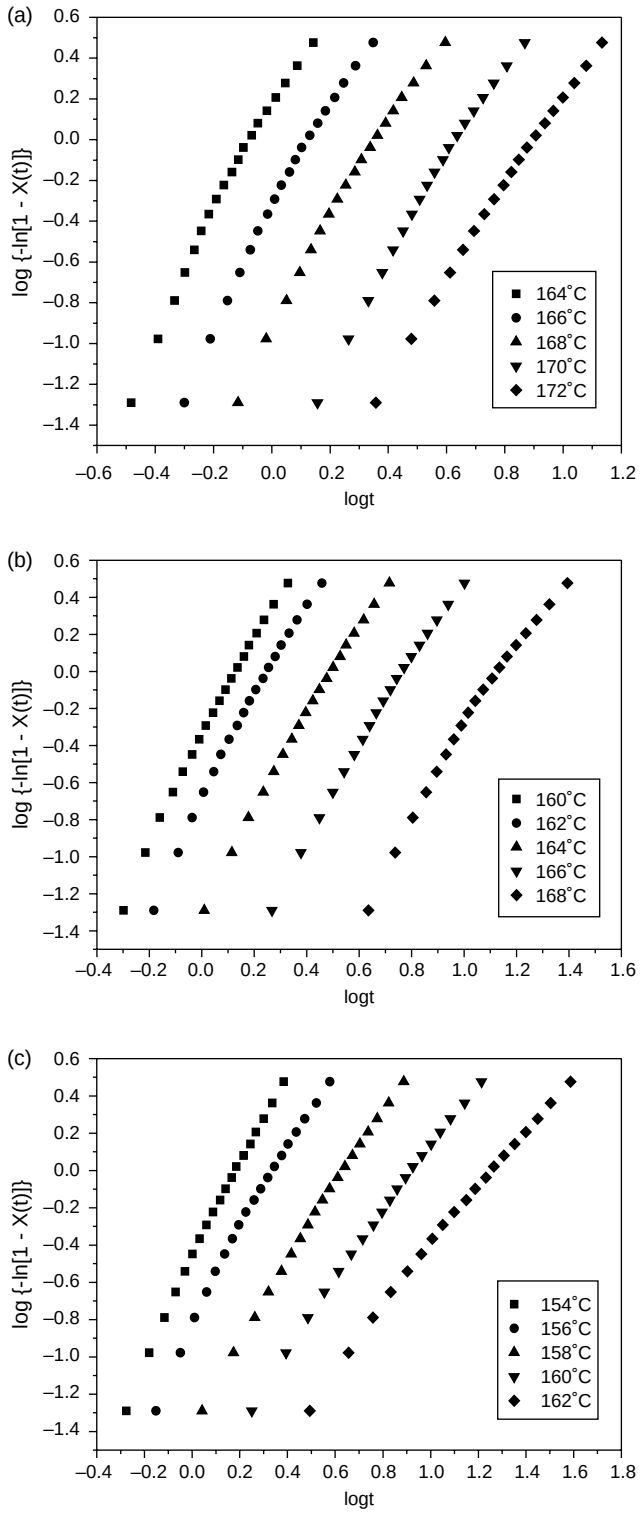

Fig. 7. Plots of $\log\{-\ln[1-X(t)]\}$ versus $\log t$ at the indicated temperature for the isothermal crystallization of samples: (a) N-0A; (b) N-5A; (c) N-10A.

from the slope and intercept, respectively, as shown in Fig. 7. It can be seen that each curve shows almost linear relationship, indicating that the Avrami equation can properly describe the isothermal crystallization behavior of samples. Each curve shows an initial linear portion, and then subsequently tends to level off. This deviation is probably attributable to the secondary crystallization, which is caused by the spherulite impingement and perfection of internal spherulite crystallization in the later stage of the crystallization process [30,31].

From the slope and intercept of the initial linear portion in Fig. 7, the values of n and K were determined and are listed in Table 1. The obtained Avrami exponent n ranges from 1.882 to

Table 1
Avrami kinetic parameters from the Avrami equation for the isothermal crystallization of samples

Sample	T_c (°C)	n	K (min^{-1})	t_{max} (min)	$t_{1/2}$ (min)	$X(t_{max})$ (%)
N-0A	164	3.334	2.333	0.697	0.695	50.361
	166	3.219	0.492	1.110	1.112	49.766
	168	2.919	0.116	1.812	1.845	48.081
	170	2.841	0.0200	3.402	3.483	47.775
	172	2.466	0.00667	6.177	6.574	44.809
N-5A	160	3.251	0.480	1.119	1.120	49.914
	162	3.165	0.230	1.468	1.474	49.511
	164	2.763	0.0500	2.513	2.590	47.158
	166	2.659	0.0100	4.733	4.924	46.421
	168	2.594	0.00160	9.915	10.386	45.975
N-10A	154	2.964	0.351	1.239	1.258	48.419
	156	2.865	0.145	1.689	1.726	47.893
	158	2.231	0.0423	3.162	3.502	42.382
	160	1.955	0.0180	5.411	6.472	38.624
	162	1.882	0.00608	10.061	12.386	37.424

3.334, indicating that there was an average contribution of simultaneous occurrence of various types of nucleation and growth of crystallization. The crystallization mode of nylon 11 might be the mixture with two-dimensional, three-dimensional, and diffusion-controlled growth with thermal nucleation. The higher the temperature, the slower the homogeneous nucleation and crystal growth rates become. So the values of n, depended on the type of nucleation and growth of the crystals, decrease with increasing crystallization temperature, as shown in Table 1. In addition, the exponent n of alloys is lower than that of neat nylon 11, because the existence of nylon 66 is unfavorable for nylon 11 to lower the crystallization, which may cause the fewer crystal defects [32]. The values of the crystallization rate parameters K increase with decreasing crystallization temperature (Table 1).

Another important parameter is the half-time of crystallization $t_{1/2}$, which is defined as the time, at which the extent of crystallization taken from the onset of the crystallization until 50% completion and can be determined from the measured kinetics parameters, as follows:

$$t_{1/2} = \left(\frac{\ln 2}{K}\right)^{1/n} \tag{3}$$

The dependency of $t_{1/2}$ on the crystallsization temperature is shown in Fig. 8. In all samples, $t_{1/2}$ increases with increasing T_c. The values of $t_{1/2}$ of alloys are higher than those of neat nylon 11, and increase dramatically with an increase of nylon 66 contents. The higher the values of $t_{1/2}$, the lower the rate of crystallization. The values of $t_{1/2}$ are listed in Table 1, indicating that the alloys have lower rate of crystallization than that of neat nylon 11. In the similar study, reduced crystallization rates have been observed in PP-cats [33], PP/PBI [34] and PEH/PEB [35] blends because of the partial miscibility.

Lin CC [36] used Eq. (1) to calculate the necessary time for maximum crystallization $X(t_{max})$ since this time corresponds to the point where $dQ(t)/dt = 0$, where $Q(t)$ is the heat flow rate.

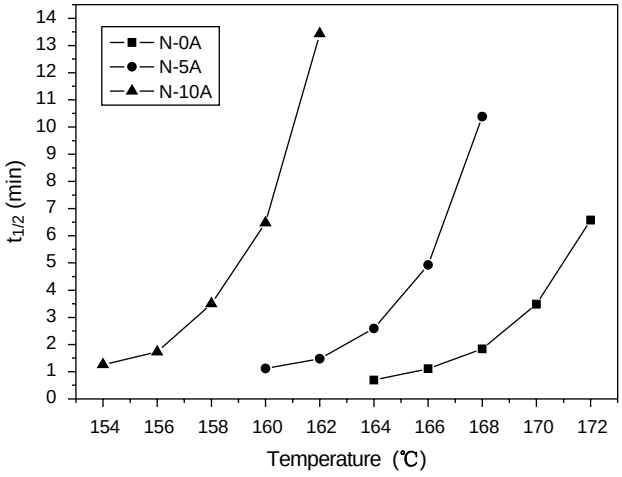

Fig. 8. Crystallization half-time as a function of crystallization temperature for samples.

t_{max} is defined by the following:

$$t_{max} = \left(\frac{n-1}{nK}\right)^{1/n} \tag{4}$$

Table 1 presents the values of n and K determined from the initial linear portions of the curves given in Fig. 7, the calculated values of t_{max}, $t_{1/2}$ and $X(t_{max})$ are also listed in Table 1, there into, the values of $X(t_{max})$ are normalized the contents of nylon 66 component.

3.3. Crystal morphology

The crystal morphologies of samples by POM are shown in Fig. 9. In order to observe and compare with the crystal morphology of samples clearly during the isothermal crystallization process, we choose the middle temperature of the range of isothermal crystallization experiment to observe by means of POM. The sample N-0A, N-5A and N-10A isothermally crystallized for 2 h at the temperature of 166, 162 and 158 °C, respectively. The N-0A displays the usual spherulite structure typified by the Maltese cross. The spherulites developed during this period are sheaf-like (the general spherical shape is little), which are usually observed only in the early stages of polymer crystallization. The spherulites impinge and the so-called second crystallization process is clearly observed. However, upon close examination, the dimension of spherulites decreased dramatically with the presence of nylon 66. In sample N-10A, typical spherulites could hardly be observed.

From a comparison of the three photographs, nylon 11 contains relatively large crystals, whereas a dense granular texture of crystals is formed in the presence of nylon 66 and the size of spherulite becomes smaller. It is clear that the number of nuclei was increased and the growth rate of the spherulites was decreased by the addition of nylon 66, considering the results of Fig. 10. It suggests that small imperfect crystallites mainly form when the mobility of the polymer chains was restricted [37]. The nylon 66 permeated in nylon 11 matrix and its chains tangled with nylon 11. It may play a role of increasing

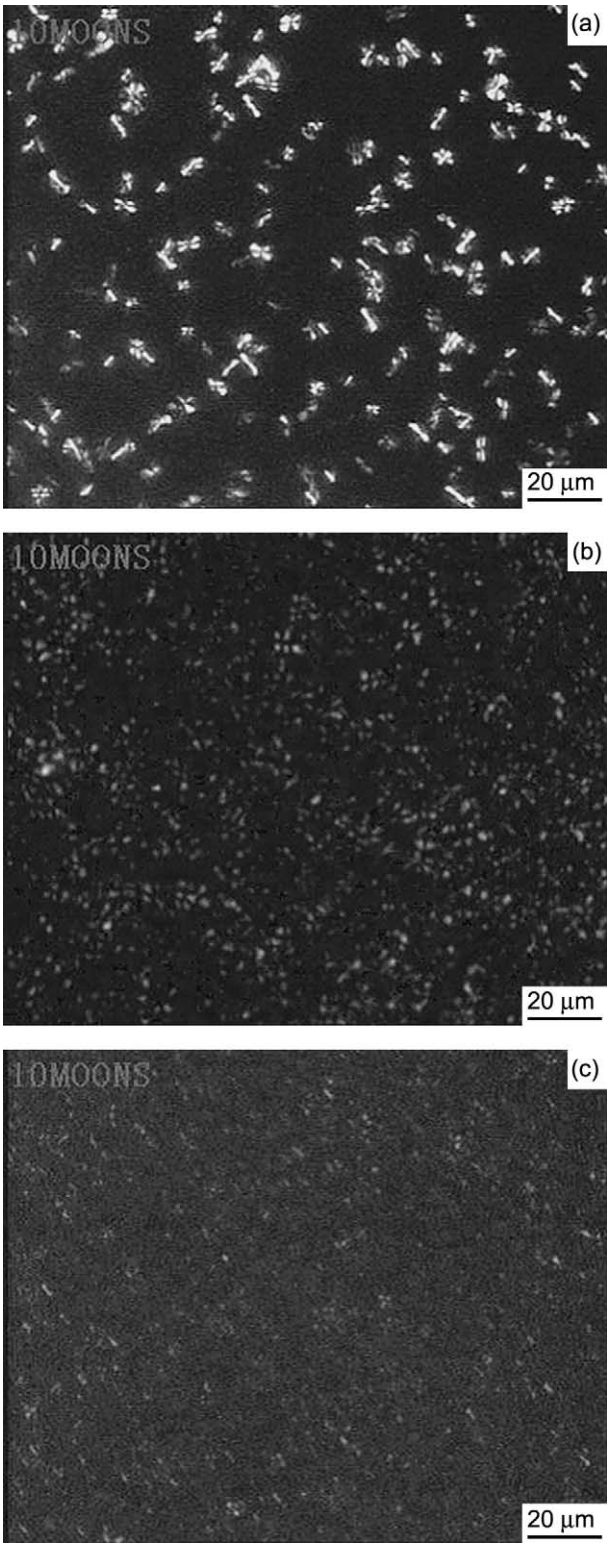

Fig. 9. Crystal morphology of samples by POM: (a) N-0A, observed at 166 °C; (b) N-5A, observed at 162 °C; (c) N-10A, observed at 158 °C.

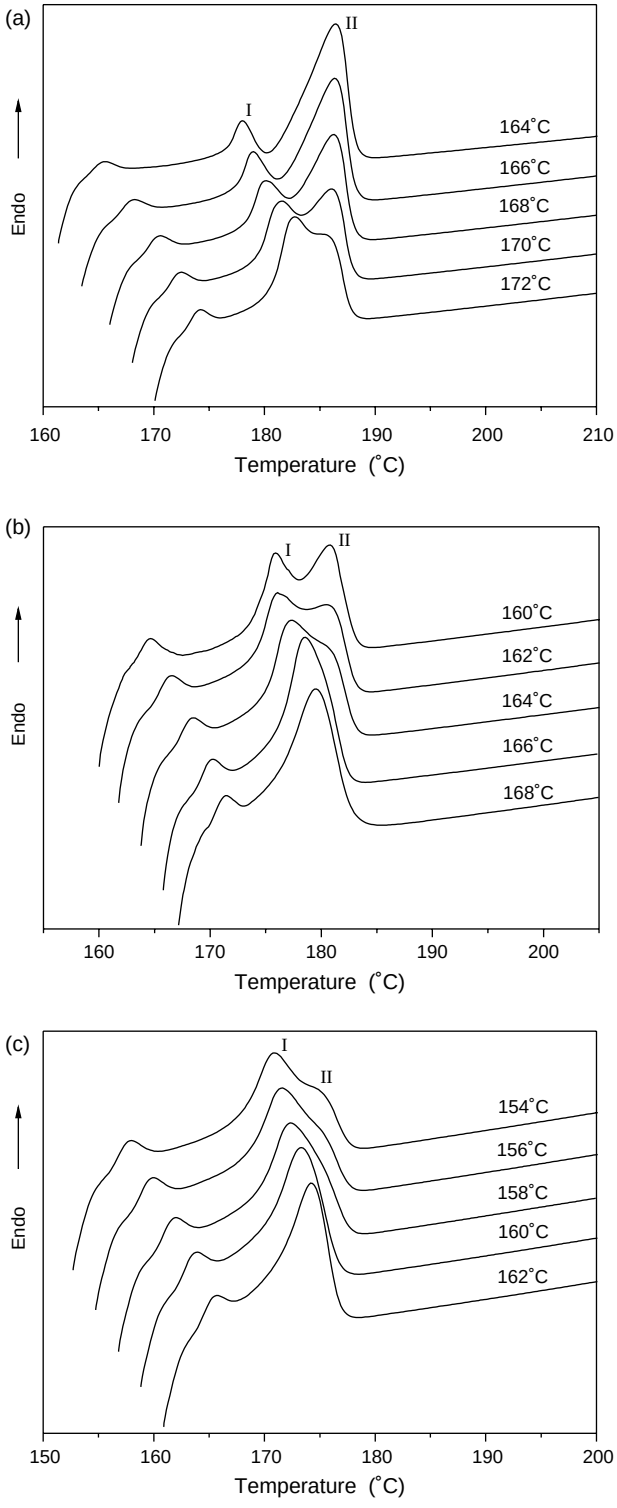

Fig. 10. The DSC thermograms of samples after isothermal crystallization at indicated temperature for 30 min at a heating rate of 10 °C/min: (a) N-0A; (b) N-5A; (c) N-10A.

the nucleation sites, in which the crystallization rate and dimension of spherulites was effected. In addition, in the case of nylon polymer, the hydrogen bonding occurs not only at the ends of the chains but also at the middle of the chains, so strong interaction will exist between nylon 11 and nylon 66; furthermore, the density of hydrogen bonding for nylon 66 is higher than that for nylon 11, strong interaction also exists in alloys; thus leading to the formation of small and highly imperfect crystalline structure, and to lowering the crystallization of nylon 11 [38]. Strong evidence for the formation of

such dimers in a long alkanoic acid has been reported by Zeng [39] and Li [40].

3.4. Melting behaviors following isothermal crystallization

The heating DSC curves of samples after isothermal crystallization at indicated temperature are shown in Fig. 10. It is clear that the entire DSC curves exhibit multiple melting peaks at the high-temperature side. Henceforth, the peak at the lower temperature is called peak I, whilst that at the higher temperature is called peak II. The peak I shifts to a higher temperature as the crystallization temperature increases. On the contrary, the peak II becomes smaller as increasing the crystallization temperature, but its position in the temperature scale remains almost constant. The multiple melting behavior of nylon 11 can be attributed to recrystallization phenomena during heating process [41,42]. Thus, the cause of the peak I in the scans is due to the melting of the material crystallized at each temperature, while the peak II corresponds to the melting of the recrystallization materials [40]. With an increase of the isothermal crystallization temperature, the crystals become thickened and more perfect, so the temperature of peak I is enhanced. Upon heating, the less stable crystals melt to a supercooled state in which recrystallization can take place very rapidly with the formation of better crystals. The final melting of recrystallized material takes place at the same temperature, regardless of the isothermal crystallization temperature at which the crystals are originally formed [2]. As a matter of fact, with increasing T_c, the originally grown crystals improve their degree of perfection up to a point where no further recrystallization can occur during the DSC run and the peak II temperature endotherm disappears.

An endothermic peak close to the isothermal crystallization temperature (at about T_c+3 °C) is also shown in Fig. 10, this phenomenon is believed to be due to the annealing effects in the crystallization process [43,44]. In addition, to the major population of lamellar crystals developed during isothermal crystallization, a small fraction of the polymer, initially ejected as noncrystallized materials between bundles of lamellae, formed as thin and very defective crystal aggregates at later stages. Upon heating, they produce the melting peaks a few degrees above the isothermal crystallization temperature.

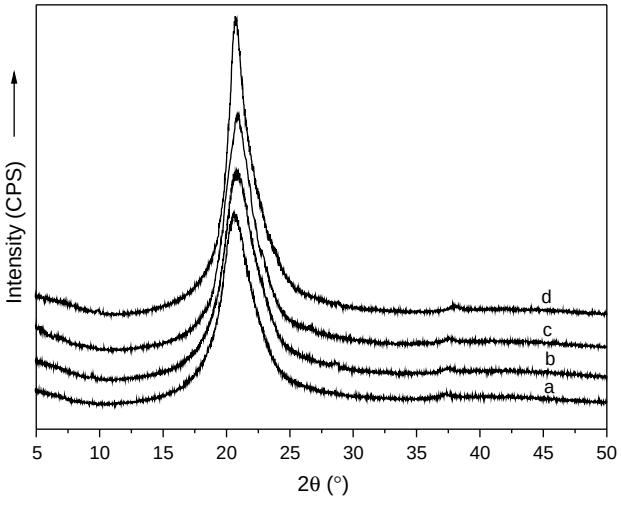

Fig. 11. The XRD patterns of N-0A isothermally crystallized at 166 °C for different time: (a) 5 min; (b) 10 min; (c) 20 min; (d) 30 min.

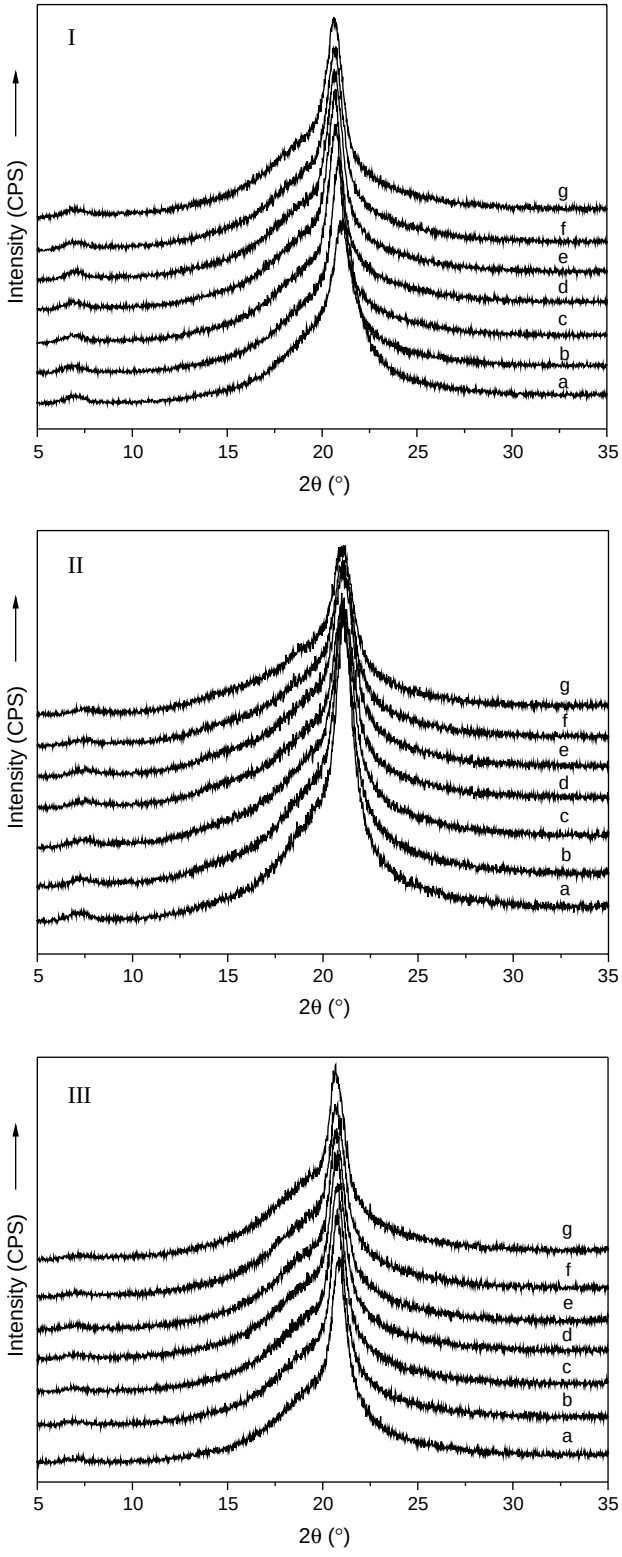

Fig. 12. The XRD patterns of samples isothermally cryatallized at different temperature: (a) 120 °C; (b) 140 °C; (c) 150 °C; (d) 155 °C, (e) 160 °C; (f) 165 °C; (g) 170 °C. I: N-0A; II: N-5A; III: N-10A.

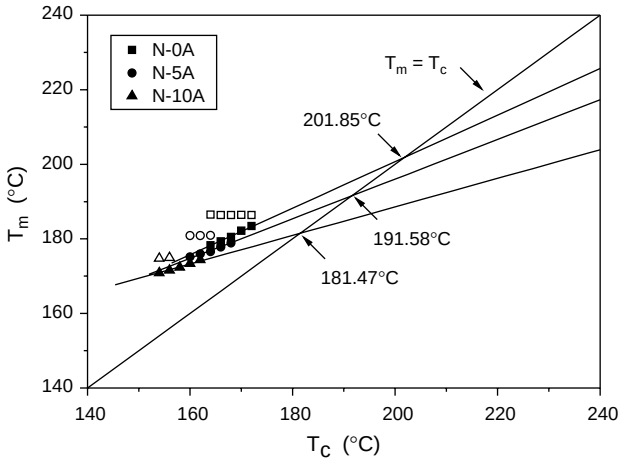

Fig. 13. Application of the Hoffman–Weeks approach to samples for determining: the corresponding blank symbols represent the temperature of peak II.

Apparently, the temperatures of peak I and II decrease with increasing nylon 66 contents, indicating that nylon 66 has great influence on the crystallization of nylon 11. The more contents the nylon 66, the more influence on crystallization of nylon 11. So it is difficult to recrystallize into perfect and stable crystals for nylon 11, and the melting temperature of recrystallized material shifts to lower temperature. Meanwhile, the peak I is more significant in N-5A and N-10A, indicating less secondary crystallization growth taken place during isothermal crystallization. This is in consistent with the results of the isothermal crystallization kinetics using Avrami theory. The similar study was reported in PVDF/Nylon11 [45] and HDPE/iPP [46].

The melting behavior of polymer crystallized has been studied in a number of different ways. A common feature of all these investigations has been the observation of multiple fusion endotherms. It is well known that aliphatic nylons can crystallize into different crystal structures, which can exhibit different melting temperature. Therefore, the multiple melting behaviors of some nylons were attributed to melting of different crystal forms or crystalline transitions during heating [47]. No crystalline transition can be observed in the melting range of samples, as shown in Figs. 11 and 12. X-ray diffractograms were recorded in rang of time and isothermal crystallization temperature. The diffraction patterns show the same reflection at high temperature, corresponding to the (100) crystal plane [14]. This indicates that only one crystal structure exists in samples during its isothermal crystallization and melting process. Therefore, the possibility that the multiple endotherms resulted from different crystalline forms can be ruled out. It is in agreement with the report by Yadav [48].

3.5. Equilibrium melting point (T_m^0)

To carry on with quantitative analysis of crystallization behavior, especially to investigate the temperature dependence of the crystallization rate, it is necessary to determine the equilibrium melting point as accurately as possible.

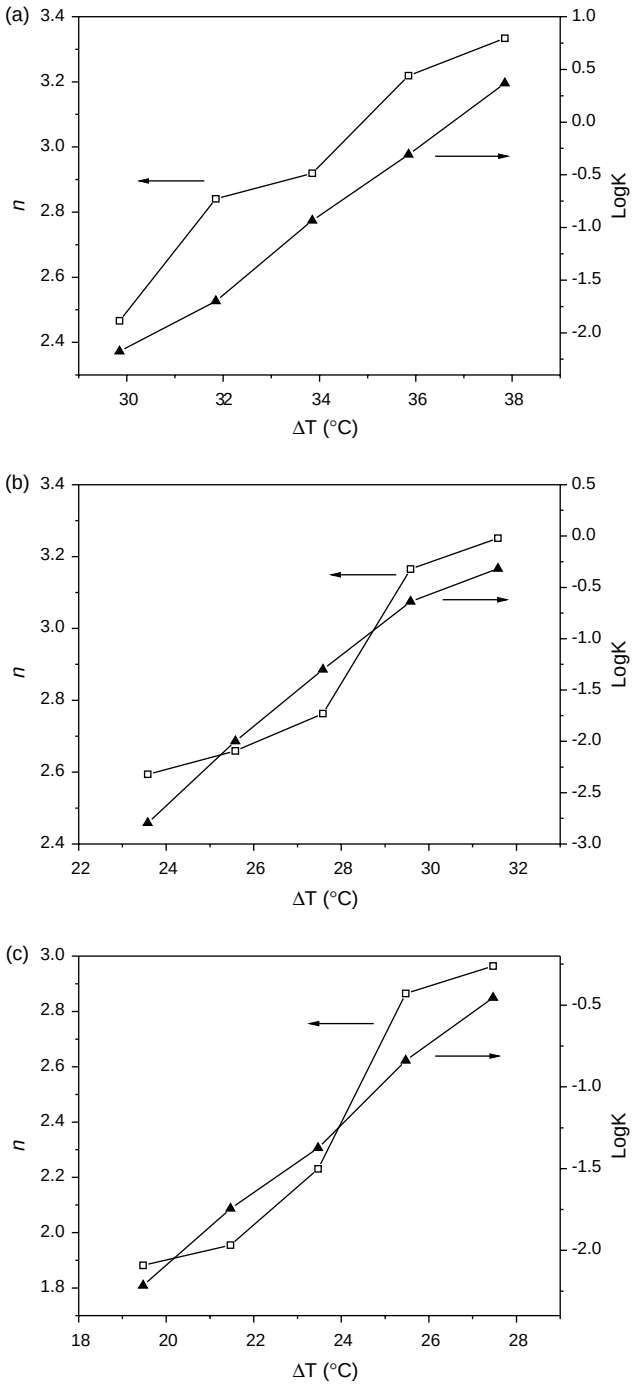

Fig. 14. The plots of n versus ΔT and log K versus ΔT: (a) N-0A; (b) N-5A; (c) N-10A.

The reliable estimate of the equilibrium melting point can be made by careful DSC studies. According to Hoffman–Weeks theory [49], the equilibrium melting point may be deduced by plotting the observed apparent melting temperature (T_m) against the crystallization temperature (T_c). The equilibrium melting point is obtained by extrapolation of the resulting straight line to intersect the line $T_m = T_c$. Assuming chain folding during crystallization, the dependence of the apparent melting temperature T_m on the crystallization temperature T_c is

expressed as:

$$T_m = T_m^0\left(1-\frac{1}{2\beta}\right)+T_c\frac{1}{2\beta} \quad (5)$$

where T_m^0 is the equilibrium melting point; β is a parameter which depends on the lamellar thickness, more precisely $\beta = l/l^*$, where l and l^* are the thickness of the grown crystallite and of the critical crystalline nucleus, respectively, [50]. It has been pointed that Eq. (5) correctly represents experimental data only when β is constant and the slope of the curve in the T_m versus T_c plot is approximately equal to 0.5 [50].

It is well known that the higher the crystallization temperature, the more suitable it is to get the equilibrium melting point [51]. At higher T_c, the β describes the growth of the lamellar thickness and is supposed to be always being greater than or equal to 1, and the slope of the plot was 0.5, so the peak I and II temperatures as a function of T_c are plotted in Fig. 13 for samples. In Fig. 13, the linear extrapolation of the experimental data up to $T_m = T_c$ line is also drawn, and the values of 201.85, 191.58, 181.47 °C for sample N-0A, N-5A and N-10A, respectively, of T_m^0 was obtained. This result of nylon 11 is in good agreement with that reported in the literature [52].

The extrapolation of T_m versus T_c (Fig. 13) shows that the melting temperature data corresponding to the lower endotherm are aligned with those obtained when only one melting peak is observed. However, the high-temperature peaks are at approximately the same position, regardless of the temperatures at which the samples were crystallized. This behavior suggests that melting and recrystallization occurs during heating [42].

In addition, the crystallization of polymer is usually considered to be the influence of the degree of supercooling. So the plots of n versus ΔT or log K versus ΔT should be the one linear relation. The plots of n versus ΔT and log K versus ΔT for all samples are shown in Fig. 14. It can be seen that the values of n for all samples does not show a good linear relation against ΔT, indicating that the presence of nylon 66 also influenced on the crystallization of nylon 11 greatly. It is in agreement with the above results.

4. Conclusions

Investigations on polymer crystallization behaviors and crystal morphology were carried out on nylon 11/nylon 66 alloys formed by in situ polymerization. The Avrami equation could be used to describe the primary stage under isothermal conditions of nylon 11 and nylon 11/nylon 66 alloys. The data obtained from the analysis of isothermal process show that nylon 66 influenced on the crystallization of nylon 11. The more the contents of nylon 66, the more influence on the crystallization of nylon 11. Polarized optical microscopy experiments also confirmed this result.

Both neat nylon 11 and nylon 11/nylon 66 alloys exhibited multiple melting behaviors after isothermal crystallization at the indicated crystallization temperature. The temperature of the lower melting peak (peak I) resulting from the melting of lamellae with different perfectness under different conditions, and the highest melting temperature (peak II) originating from the melting of the recrystallized crystals, both decreased with increasing nylon 66 contents. The equilibrium melting point for isothermal crystallization of samples had also been evaluated according to the classical theory.

Acknowledgements

This work was supported by the National '973' Project (Contract No.2003CB615602). The authors acknowledge with gratitude the support from Shanghai Genius Advanced Materials Co., Ltd.

References

[1] Fatou JG. Encyclopedia of polymer science and engineering. New York: Wiley; 1989. Suppl. 231.
[2] Lu XF, Hay JN. Polymer 2001;42:9423.
[3] Di Lorenzo ML, Silvestre C. Prog Polym Sci 1999;24:917.
[4] Mehrabzadeh M, Burford RP. J Appl Polym Sci 1996;61:2305.
[5] Slichter WP. J Polym Sci 1959;36:259.
[6] Little K, Phil MAD. J Polym Sci 1959;10:225.
[7] Kawaguchi A. J Macromol Sci Phys 1981;20:1.
[8] Kim KG, Newman BA, Scheinbeim JI. J Polym Sci Polym Phys 1985; 23:2477.
[9] Newman BA, Sham TP, Pae KD. J Appl Phys 1977;48:4092.
[10] Greco R, Nicolais L. Polymer 1976;17:1049.
[11] Yoshiyuki T, Masataka T, Masayuki K, Takeo F. Polym J 1997;9:34.
[12] Yu HH. Mater Chem Phys 1998;56:289.
[13] Zhang QX, Mo ZS, Liu SY, Zhang HF. Macromolecules 2000;33: 5999.
[14] Zhang QX, Mo ZS, Zhang HF, Liu SY, Cheng SZD. Polymer 2001; 42:5543.
[15] Rhee S, White JL. J Polym Sci, Part B: Polym Phys 2002;40:2624.
[16] Chocinski-Arnault L, Gaudefroy V, Gacougnolle JL. J Macromol Sci, Part B: Phys 2002;41:777.
[17] Mehrabzadeh M, Burford RP. J Appl Polym Sci 1997;64:1605.
[18] Deimede VA, Fragou KV, Koulouri EG, Kallitsis JK, Voyiatzis GA. Polymer 2000;41:9095.
[19] Hu GS, Wang BB, Zhou XM. Polym Int 2005;54:316.
[20] Genas M. Angew Chem 1962;74:535.
[21] Mubarak Y, Harkin-Jones EMA, Martin PJ, Ahmad M. Polymer 2001;42: 3171.
[22] Finelli L, Lotti N, Munari A. Eur Polym Sci 2001;37:2039.
[23] Gurato G, Fichera A, Grandi FZ, Zannetti R, Canal P. Macromol Chem 1974;175:953.
[24] Medellin-Rodriguez FJ, Larios-Lopez L, Zapata-Espinoza A, Davalos-Montoya O, Phillips PJ, Lin JS. Macromolecules 2004;37:1799.
[25] Medellin-Rodriguez FJ, Phillips PJ, Lin JS, Campos R. J Polym Sci, Part B: Polym Phys 1997;35:1757.
[26] Avila-Orta CA, Medellin-Rodriguez FJ, Wang ZG, Navarro-Rodriguez D, Hsiao BS, Yeh F. Polymer 2003;44:1527.
[27] Cebe P, Hong SD. Polymer 1986;27:1183.
[28] Avrami M. J Chem Phys 1939;7:1103.
[29] Shultz J. Polymeric materials science. New York: Prentice-Hall; 1974.
[30] Wunderlich B. Macromolecular physics, vol. 2. New York: Academic Press; 1977.
[31] Liu JP, Mo ZS. Chin Polym Bull 1991;4:199.
[32] Kilwon C, Fengkui L, Jaeseung C. Polymer 1999;40:1719.
[33] Zheng Q, Shangguan YG, Yan SK, Song YH, Peng M, Zhang QB. Polymer 2005;46:3163.

[34] Thomann R, Kressler J, Rudolf B, Mulhaupt R. Polymer 1996;37:2635.
[35] Wang ZG, Wang H, Shimizu K, Dong JY, Hsiaod BS, Han CC. Polymer 2005;46:2675.
[36] Lin CC. Polym Eng Sci 1983;23:113.
[37] Everaert V, Groeninckx G, Koch MHJ, Reynaers H. Polymer 2003; 44:3491.
[38] Barham PJ, Jarvis DA, Keller A. J Polym Sci Polym, Phys Ed 1982; 20:1733.
[39] Zeng X, Ungar G. Macromolecules 1999;32:3543.
[40] Li J, Organ SJ, Hobbs JK, Terry AE, Barham PJ, Seebach D. Polymer 2004;45:8913.
[41] Li YJ, Zhu XY, Tian GH, Yan DY, Zhou EL. Polym Int 2001;50:677.
[42] Lee Y, Porter RS, Lin JS. Macromolecules 1989;22:1754.
[43] Wunderlich B. Macromolecular physics, vol. 3. New York: Academic Press; 1980.
[44] Liu M, Zhao Q, Wang Y, Zhang C, Mo Z, Cao S. Polymer 2003;44:2537.
[45] Li YJ, Kaito A. Polymer 2003;44:8167.
[46] Na B, Wang K, Zhao P, Zhang Q, Du RN, Fu Q, et al. Polymer 2005; 46:5258.
[47] Ishikawa T, Nagai S. J Polym Sci, Polym Ed 1980;18:1413.
[48] Yadav YS, Jain PC. Polymer 1986;27:721.
[49] Hoffman JD, Weeks JJ. J Res Natl Bur Stand 1962;66A:13.
[50] Alamo RG, Viers BD, Mandelkern L. Macromolecules 1995;28:3205.
[51] Wang GM, Yan DY, Bu HS. Chin J Polym Sci 1998;16:2642.
[52] Liu SY, Yu YN, Cui Y, Zhang HF, Mo ZS. J Appl Polym Sci 1998; 70:2371.